

## A model of the steam compression process in a piston reactor

DAMIAN JOACHIMIAK<sup>a\*</sup>  
TOMASZ BOROWCZYK<sup>b</sup>  
MAGDA JOACHIMIAK<sup>a</sup>

<sup>a</sup> Poznan University of Technology, Institute of Thermal Engineering, Piotrowo 3a, 60-965, Poznań, Poland

<sup>b</sup> Grupa inżynierska Konstrubowski Sp. z o.o., Święty Wojciech 7/13, 61-749 Poznań, Poland

**Abstract** The paper discusses the possible determination of steam parameters in a new type of piston machine for steam compression to generate supercritical water parameters. It presents a calculation model that allows one to simulate the process of steam compression in a cylinder with volume regulated by the piston position. In each calculation step, the steam parameters were determined on the basis of fast adiabatic changes which were corrected by the effect of leakage and heat transfer occurrence. The seal of the reactor was assumed to be a compression ring. Depending on the pressure drop on the seal, subcritical and supercritical flow was taken into account. The leak was corrected by the coefficient of flow contraction. Heat transfer was determined by equations for the Nusselt number for water and steam from the homogenous area. The programmed model allows one to simulate changes in the thermodynamic parameters of steam during the process of steam compression with any calculation step. The results presented in this paper show that the application of one compression ring allows us to obtain supercritical steam parameters. Various degrees of sealing leak tightness and their impact on the changeability of steam parameters were analyzed. Heat transfer was shown to have an impact not only on changes in steam temperature, but also on pressure. This paper analyzes the impact of the temperature of the walls of the compression chamber on the value and direction of heat transfer.

---

\*Corresponding Author. Email: [damian.joachimia@put.poznan.pl](mailto:damian.joachimia@put.poznan.pl)

**Keywords:** Steam; Critical water parameters; Piston-cylinder system; Compression rings; Thermodynamic parameters; Piston reactor; Heat transfer

## Nomenclature

$A$	–	area, $\text{m}^2$
$a$	–	speed of sound, $\text{m/s}$
$c_{\text{pis}}$	–	speed of piston, $\text{m/s}$
$c_p$	–	specific heat capacity at constant pressure, $\text{J}/(\text{kgK})$
$c_v$	–	specific heat capacity at constant volume, $\text{J}/(\text{kgK})$
$D$	–	cylinder diameter, $\text{m}$
$F$	–	force, $\text{N}$
$H$	–	height, $\text{m}$
HT	–	parameter including heat transfer
$h$	–	specific enthalpy, $\text{J}/\text{kg}$
$i$	–	iteration, calculation step
$m$	–	mass, $\text{kg}$
$\dot{m}$	–	mass flux, $\text{kg/s}$
$p$	–	pressure, $\text{Pa}$
$R$	–	individual gas constant, $\text{J}/(\text{kgK})$
Re	–	Reynolds number
$s$	–	entropy, $\text{J}/(\text{kgK})$
$T$	–	temperature, $\text{K}$
$t$	–	time, $\text{s}$
$V$	–	volume, $\text{m}^3$
$v$	–	specific volume, $\text{m}^3/\text{kg}$
$x$	–	steam dryness
$z$	–	piston displacement, $\text{m}$

## Symbols for calculation variants

HT0	–	exclusion of heat transfer from steam to wall
HT1	–	inclusion of heat transfer from steam to wall
L0	–	exclusion of leakage
$Li$	–	inclusion of leakage by $i$ -times of the reference flow area in the piston ring gap $A_{\text{RG}}$

## Greek symbols

$\alpha$	–	heat transfer coefficient, $\text{W}/(\text{m}^2\text{K})$
$\Delta$	–	elementary growth
$\delta$	–	relative value
$\kappa$	–	isentropic exponent
$\lambda$	–	heat conductivity coefficient, $\text{W}/(\text{mK})$
$\mu$	–	dynamic viscosity, $\text{kg}/(\text{ms})$
$\nu$	–	kinematic viscosity, $\text{m}^2/\text{s}$
$\rho$	–	density, $\text{kg}/\text{m}^3$

**Subscripts**

cyl	–	cylinder parameter
g-w	–	parameter expressing heat transfer between steam and cylinder walls
l	–	leakage
pis	–	piston
RG	–	ring gap
sum	–	sum
w	–	wall

**1 Introduction**

Water, in its subcritical and supercritical state, can be used in chemical synthesis reactions, nanoparticles production, hydrothermal liquefaction and gasification [1,2]. High pressure (more than 22 MPa) and temperature (more than 375°C) of steam constitute technological and economic barriers to its common use [3]. An advantage of a piston reactor is that it can be used to obtain high steam parameters with relatively simple constructional solutions and small investment expenditures [4]. Moreover, it can minimize the time of the chemical reaction, thus providing higher process performance. The impact of a flow nature, described by the Reynolds number, in a continuous supercritical water gasification reactor was investigated in the paper [5]. An increase in the Re number from the laminar flow to the turbulent flow allows a reduction of the gasification time of ethanol and butanol. In the paper [6] a piston engine is treated as a chemical reactor. The impact of the preliminary move of substrates on the process of combustion in a diesel engine was examined. In paper [7] a concept of using the piston-cylinder assembly of a single-stroke rapid compression machine and the piston engine as a chemical reactor was presented.

Depending on the type of machine, operating medium and working conditions, different types of seal are used in piston-cylinder assemblies. In piston compressors with relatively low values of the compression ratio obtained in a single degree non-contact labyrinth groove seals are used [8]. Application of relatively large radial clearance in a non-contact piston-cylinder seal may cause gas expansion not to occur in the constrictions. And this will result in excessive leakage [9]. To minimize leakage in non-contact labyrinth seals in the piston-cylinder assembly, the radial clearances of less than 0.1 mm are used. A seal of this type requires a system to guide

the piston in the cylinder liner. In the paper [10], research on leakage and pressure distribution of the labyrinth seal geometry in a piston compressor with a low pressure drop of 3.2 bar. The results of numerical research on air flow in the piston-cylinder seal are included in the paper [11]. The impact of the seal geometry, that is, of tooth thickness, chamber size, and of the clearance in a labyrinth seal, on the leakage rate is analyzed there. The application of the labyrinth seal to a conceptual engine with a free piston is described in [12]. The results presented there indicate a lower engine efficiency caused by greater leakage compared to the conventional seal with lubricated piston rings. The use of non-contact seals allows oil to be eliminated from the surface of the cylinder liner. Another type of seal, which can be used in piston-cylinder systems, are slot seals. This type of seal can be applied in the case of a very small radial clearance. In slot seals, leakage is reduced by tangential tensions between the fluid and the seal walls [13]. The method to determine the leakage in the radial slot seal is presented in the paper [14]. This method is based on experimentally determined flow coefficients that are a function of the height of clearance. The paper [15] includes the description of the method for calculating the leakage in this type of seal, taking into account the geometry of the channel of the inlet section. The paper [16] includes the description of a generalized model based on the Stodola equation. This model enables determining the leakage for liquids and gases and for compressible and incompressible flows in the groove seal channels. The calculation model that allows for the determination of gas leakage and the distribution of thermodynamic parameters in a slot seal is presented in [17]. In this model, an irreversible adiabatic transition is assumed with dissipation of kinetic energy to frictional heat. The friction coefficient was determined using the corrected Blasius equation. Labyrinth seals in the piston-cylinder assembly are widely used. The paper [18] presents an optimally designed labyrinth seal on the 10 K G-M refrigerator displacer. Various clearance values were experimentally analyzed. Analysis of the impact of cavity width and depth, tooth thickness, and seal clearance on leakage in a piston compressor seal is discussed in [11]. The problem of optimizing labyrinth seals, which can be used in piston-cylinder seals, was described in the paper [19]. It comprises the analysis of the impact of a chamber geometry on the value of liquid leakage. Furthermore, a semi-theoretical model with two new parameters, which are the virtual cavity velocity and the vortex loss coefficient, was presented in it. The paper [20] comprises the analysis of gas flow in the labyrinth seal with an increasingly smaller pitch until the geometry of a slot seal is obtained. The

impact of pitch on leakage and pressure distribution in the seal was investigated there. A numerical analysis of leakage and discharge coefficients in staggered labyrinth seals was presented in [21]. The effect of changing the seal geometry on a decrease in the discharge coefficient was studied. The paper [22] includes a new approach to the design of labyrinth seals that consists of matching the geometry of the seal with the flow conditions. A novelty is adjusting the number and arrangement of teeth and chambers geometry to distribution of the gas kinetic energy in the clearances to obtain as great a degree of energy dissipation in the chambers as possible. The paper [23] presents a numerical study of supercritical carbon dioxide flow in a labyrinth seal consisting of a varying number of teeth. The impact of the number of teeth on the leakage rate was analyzed.

Contact seals with compression rings are commonly used in piston-cylinder assemblies. In the literature, there are some descriptions of computational models for such seals. In the paper [24] a one-dimensional calculation model of the sealing system of a Stirling engine with a free piston is presented. The working medium was helium. A seal consisting of a sealing ring was analyzed. The flow through the sealing ring was assumed to be an incompressible flow. The calculations were discretized every 10 degrees of the crankshaft rotation angle. In the paper [25] a two-dimensional CFD model of the transport of a mass through the crevices of the piston liner in a diesel engine was presented. The leak through the annular gaps is determined analytically and included in the CFD model. In the paper [26] a gas leakage model was discussed, as well as the model of displacing and lubricating rings in a piston-ring-cylinder assembly. In these models, steam was not used as a working medium.

This paper presents a calculation model for the steam compression process in a piston reactor. The main aim of developing this model is to analyze the obtainable thermodynamic parameters, such as steam pressure and temperature, for various variants of the calculations. Results from the calculations will enable verification of obtained peri-critical parameters of steam, and thus they will show if it is possible to create conditions enabling the reaction of hydrothermal gasification to occur. The leakage of the operating medium in the piston-cylinder seal has a direct impact on the obtainable steam parameters. As the subject of this study is the concept of a new-type machine, various types of sealing will be considered during the machine construction. At the stage of a machine design, application of non-contact labyrinth seals should be considered, because they do not need an oil film on the surface of the cylinder liner.

In this paper, the process of steam compression in the piston-liner assembly has been analyzed. The seal system has been assumed to consist of one piston ring (1, Fig. 1a). In such a system, there is an oil control ring below the compression ring (3, Fig. 1a). The first compression ring is primarily responsible for limiting leakage (Fig. 1b).

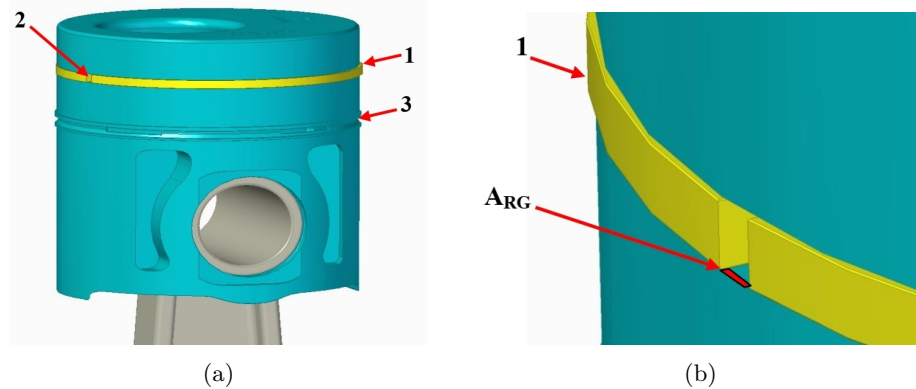


Figure 1: Piston seal system: (a) general view, (b)  $A_{RG}$  – flow reference area in the compression ring gap. 1 – compression ring, 2 – ring gap, 3 – oil control ring.

This type of seal allows a high compression ratio to be obtained; however, it requires the presence of an oil film on the surface of the cylinder liner. The tightness of the seal made up of compression rings is affected by the shape of the sliding layer, the number of rings, and the geometry of the ring gap [27].

Temperature and pressure changes of the operating medium are generally significant in piston-cylinder seals. Changes in these parameters can cause changes in viscosity, and thus changes in flow nature in the seal. The impact of the change of the viscosity parameter after the change in gas temperature in the spiral groove seal was described in the paper [28].

It is mandatory to develop a model of the steam compression process in order to design a piston reactor. In the literature, there is no calculation model that would include leakage and heat transfer for steam in the piston-cylinder assembly. This model will include steam parameters on the basis of the IAPWS-IF97 steam tables [29]. Piston position, pressure, temperature, and leakage values of the operating medium experience rapid changes over time during steam compression in a piston reactor. These parameters affect the intensity of the heat transfer from the operating medium (steam) to

the walls of the reactor compression chamber (these surfaces include the cylinder liner, head, and piston tops). The developed compression model considers the impact of heat transfer, leak tightness, and piston velocity on the thermodynamic parameters of steam in the cylinder of a piston reactor.

## 2 The main calculation model

The concept of a piston reactor shown in Fig. 2 consists of a cylinder liner (1), a piston (2), a compression chamber (3), and a valve system (4). Steam compression occurs during the movement of the piston inside the cylinder liner. The calculation model allows the compressed steam parameters to be determined with 1 mm step of the piston movement (Fig. 3). The model has been programmed in such a way as to perform theoretical calculations of the compression process:

- excluding leakage and heat transfer,
- including leakage,
- including heat transfer,
- including leakage and heat transfer.

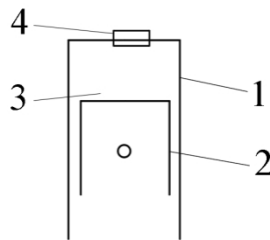


Figure 2: Piston reactor model: 1 – cylinder liner, 2 – piston, 3 – reactor chamber, 4 – valve system.

The authors' own program, ST\_IF97, was used in the calculations to determine the steam parameters. The program was written using Fortran with the inclusion of the *ASME International Steam Tables for Industrial Use* [27]. At the beginning of the calculations, the authors assumed the initial pressure of 200 kPa of the dry steam supply to the cylinder (1, Fig. 2) through the valve.

Based on the initial pressure  $p(1)$  and with the use of the ST\_IF97 program, the parameters (temperature, density, enthalpy, speed of sound, specific heat at constant pressure, specific heat at constant volume, entropy, dynamic viscosity, kinematic viscosity, heat transfer coefficient) were determined for saturated dry steam ( $x = 1$ ) at the initial position of the piston

$$p(1) \xrightarrow{\text{ST\_IF97}} T(1), \rho(1), h(1), a(1), c_p(1), c_v(1), s(1), \mu(1), \nu(1), \lambda(1). \quad (1)$$

The gas mass inside the cylinder was calculated according to the formula:

$$m_{\text{cyl}}(i) = V_{\text{cyl}}(i)\rho(i). \quad (2)$$

The isentropic exponent is changeable for steam. It was expressed by the dependency:

$$\kappa(i) = \frac{a(i)^2}{p(i)\nu(i)}. \quad (3)$$

With the calculation model, it is possible to determine the theoretical distribution of steam parameters during compression in a piston reactor at every  $i$ th calculation step.

The gas pressure for the subsequent  $i$ th calculation step (piston positions according to Fig. 3) was determined assuming a rapidly occurring isentropic transformation

$$p(i) = p(i-1) \left( \frac{V_{\text{cyl}}(i-1)}{V_{\text{cyl}}(i)} \right)^{\kappa(i-1)}. \quad (4)$$

The gas temperature for the subsequent  $i$ th calculation step (piston positions) is also determined on the basis of an isentropic transformation

$$T(i) = T(i-1) \left( \frac{p(i)}{p(i-1)} \right)^{\frac{\kappa(i-1)-1}{\kappa(i-1)}}. \quad (5)$$

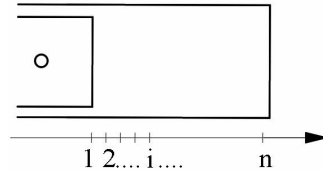


Figure 3: Calculation step.

The remaining part of the paper first describes the main part of the model with the assumed ideally sealed cylinder and without heat transfer between the steam and the cylinder walls. By controlling the model operation, it is possible to include heat transfer between the steam and the compression chamber walls, as well as steam leakage in the piston-cylinder seal. The calculation model to determine leakage values (leakage calculation model, LCM) is described in detail in Section 2.1. Data about the type and geometry of the seal were entered into the program. The flow area through the ring is crucial in the analyzed seal consisting of a compression ring. The area has been defined in the following part of the paper as the flow reference area around the ring gap and marked as  $A_{RG}$  (Fig. 1). The steam mass leaking through the seal over time of the  $i$ th calculation step  $m_l(i)$  is calculated at each calculation step, based on the current pressure, temperature, steam density and isentropic exponent, as conceptually shown below:

$$\text{sealing type, } A_{RG}, D_{cyl}, H_{pis}p(i), T(i)\rho(i), \kappa(i) \xrightarrow{\text{LCM}} \dot{m}_l(i). \quad (6)$$

The amount of gas that has leaked out of the cylinder through the seal over time  $\Delta t$ , was expressed as the following dependency

$$m_l(i) = \dot{m}_l(i)\Delta t(i). \quad (7)$$

If the velocity of the piston changes, then the value of  $\Delta t$  and  $m_l$  for each  $i$ th calculation step is different. The amount of gas in the cylinder for the  $i$ th calculation step corrected by the leakage value was expressed as the following dependency:

$$m_{cyl,l}(i) = m_{cyl}(i) - m_l(i). \quad (8)$$

Correction of the gas pressure inside the cylinder, resulting from the leakage, was determined with the assumed fast adiabatic change

$$p(i) = p(i) \left[ \frac{m_{cyl,l}(i)}{m_{cyl}(i)} \right]^{\kappa(i)}, \quad (9)$$

whereas the correction of the gas temperature inside the cylinder resulting from the change of mass inside the cylinder was expressed with the following formula:

$$T(i) = T(i) \left[ \frac{m_{cyl,l}(i)}{m_{cyl}(i)} \right]^{\kappa(i)-1}. \quad (10)$$

The next iteration assumed the steam mass value in the cylinder corrected by the leakage value

$$m_{\text{cyl}}(i) = m_{\text{cyl},l}(i). \quad (11)$$

The subsequent stage of the calculations can include the impact of the heat transfer between compressed steam and the cylinder walls on the steam parameters at each calculation step. For this purpose, parameters such as density, dynamic and kinematic viscosity, heat transfer coefficient, and the Prandtl number for steam ( $\rho(i)$ ,  $\mu(i)$ ,  $\nu(i)$ ,  $\lambda(i)$ ,  $\text{Pr}(i)$ ) were obtained from the ST\_IF97 program. The Reynolds number at the  $i$ th calculation step was determined on the basis of the momentary piston velocity:

$$\text{Re}(i) = \frac{c_{\text{pis}}(i)D_{\text{cyl}}}{\nu(i)}. \quad (12)$$

Heat is transferred between the compressed steam and the cylinder walls (including the top of the piston). A subprogram, described in Section 2.2 of the paper (heat transfer calculation model, HTCM), was used to determine the amount of heat transferred. The heat transfer coefficient for the steam and the cylinder walls was determined based on the geometry, momentary piston velocity, and steam parameters listed on the left side of formula (13):

$$D_{\text{cyl}}, h_{\text{cyl}}(i), c_p(i), \mu(i), \lambda(i), \text{Re}(i), \text{Pr}(i) \xrightarrow{\text{HTCM}} \alpha(i). \quad (13)$$

The height of the cylinder over the piston top  $H_{\text{cyl}}(i)$  was different for each calculation step. The surface area of the heat transfer was the side surface of the cylinder and the surface of the top and head of the piston, defined by the dependency

$$A_{\text{g-w}}(i) = 0.5\pi D_{\text{cyl}}^2 + \pi D_{\text{cyl}}H_{\text{cyl}}(i). \quad (14)$$

The heat contained in the gas was expressed using the formula

$$Q_{\text{cyl}}(i) = m_{\text{cyl}}(i)h(i). \quad (15)$$

The amount of heat transferred between the steam and the cylinder walls at temperature  $T_w(i)$  was calculated on the basis of the dependency:

$$Q_{\text{g-w}}(i) = \alpha(i)A_{\text{g-w}}(i) [T(i) - T_w(i)] \Delta t(i). \quad (16)$$

The decrease in gas temperature inside the cylinder was determined based on the known amount of heat transferred between the gas and the walls of

the compression chamber at the  $i$ th step  $\Delta T(i)$

$$\Delta T(i) = \frac{Q_{g-w}(i)}{m_{cyl}(i)c_p(i)}. \quad (17)$$

The gas pressure was corrected as a consequence of the change in temperature

$$p(i) = p(i) \left[ \frac{T(i) - \Delta T(i)}{T(i)} \right]^{\frac{\kappa(i)}{\kappa(i)-1}} \quad (18)$$

and then the steam temperature in the cylinder was corrected:

$$T(i) = T(i) - \Delta T(i). \quad (19)$$

Based on the data obtained, it is possible to determine the force required to move the piston (and the required power)

$$F(i) = A_{pis}p(i). \quad (20)$$

The steam parameters for the next calculation steps  $i = 2, 3, \dots, n$  were calculated in the ST\_IF97 program based on the current pressure and temperature

$$p(i)T(i) \xrightarrow{\text{ST\_IF97}} \varrho(i), h(i), a(i), c_p(i), c_v(i), s(i), \mu(i), \nu(i), \lambda(i). \quad (21)$$

Subsequently, the calculations were performed according to formulas (2)–(18). The model, along with subprograms, was written in the Fortran language.

## 2.1 Leakage calculation model

The model assumed that the seal of the piston-cylinder system consisted of a compression ring. Furthermore, leakage has been assumed to occur around the ring gap, as shown in Fig. 1.

The pressure ratio downstream and upstream of the ring was expressed as

$$\beta(i) = \frac{p_{out}}{p_0(i)}. \quad (22)$$

The model was based on the Saint-Venant equation [28], which was used to determine the leakage value around the compression ring gap

$$\dot{m}(i) = A_{RG}\Psi(i)\sqrt{p_0(i)\rho_0(i)}, \quad (23)$$

where  $A_{RG}$  was the flow reference area in the compression ring gap (Fig. 1), and  $\Psi$  was the flow number. For the subcritical flow  $\beta(i) > 0.5457$ , number  $\Psi$  was described by the dependency

$$\Psi(i) = \sqrt{2 \frac{\kappa(i)}{\kappa(i) - 1} \left[ \beta(i)^{\frac{2}{\kappa(i)}} - \beta(i)^{\frac{(\kappa(i)+1)}{\kappa(i)}} \right]} \quad (24)$$

and for the supercritical flow  $\beta(i) < 0.5457$

$$\Psi(i) = \sqrt{\kappa(i) \left( \frac{2}{\kappa(i) + 1} \right)^{\frac{(\kappa(i)+1)}{(\kappa(i)-1)}}}. \quad (25)$$

The value of leakage through the ring at  $i$ th time step was determined based on the corrected Saint-Venant equation

$$\dot{m}_l(i) = \mu(i)\dot{m}(i), \quad (26)$$

where the flow contraction coefficient related to the flow through the ring gap was described by the dependency [23]

$$\mu(i) = 0.85 - 0.25 \left( \frac{p_{out}}{p_0(i)} \right)^2. \quad (27)$$

The result value of the mass flux is exported to the main model.

## 2.2 Heat transfer calculation model

Heat transfer between steam and the walls of the cylinder is a significant phenomenon during the stem compression process. The intensity of heat transfer depends on the parameters of steam inside the cylinder and its swirl. The swirl of steam inside the cylinder is described by the Reynolds number (12). The Re number depends on the velocity of the piston, which varies over the time of compression stroke. The model assumed the diameter of the cylinder  $D_{cyl}$  as the characteristic dimension. It included equations that define the Nusselt number for steam in a homogenous area.

For the laminar motion of the steam in the cylinder  $Re < 2000$ , the following equation was used [30]:

$$Nu(i) = 1.615 \left( Re(i) Pr(i) \frac{D_{cyl}}{H_{cyl}(i)} \right)^{\frac{1}{3}}. \quad (28)$$

In the case of turbulent motion of the steam in the cylinder, for  $\text{Re} \in [10^4, 10^6]$  and  $\text{Pr} \in [0.6, 10^3]$ , the Gnielinski equation was used in the model [30]:

$$\text{Nu}(i) = \frac{\left(\frac{\xi(i)}{8}\right) \text{Re}(i) \text{Pr}(i)}{1 + 12.7 \sqrt{\frac{\xi(i)}{8}} (\text{Pr}(i)^{\frac{2}{3}} - 1)} \left[ 1 + \left(\frac{D_{\text{cyl}}}{H_{\text{cyl}}(i)}\right)^{\frac{2}{3}} \right], \quad (29)$$

where

$$\xi(i) = [1.8 \log \text{Re}(i) - 1.5]^{-2}. \quad (30)$$

The Nu number of the intermittent flow for  $\text{Re} \in [2300, 10^4]$  and  $\text{Pr} \in [0.6, 10^3]$  was defined in the following way [30]:

$$\text{Nu}(i) = (1 - \gamma) \text{Nu}_{\text{lam},2300}(i) + \gamma \text{Nu}_{\text{turb},10^4}(i), \quad (31)$$

where

$$\gamma(i) = \frac{\text{Re}(i) - 2300}{10^4 - 2300}(i). \quad (32)$$

The  $\text{Nu}_{\text{lam},2300}$  value was determined using Eq. (28) for  $\text{Re} = 2300$  and the  $\gamma \text{Nu}_{\text{turb},10^4}(i)$  value was determined using the Gnielinski equation (29)–(30) for  $\text{Re} = 10^4$ .

The heat transfer coefficient was determined on the basis of the Nusselt number

$$\alpha(i) = \frac{\text{Nu}(i) \lambda(i)}{D_{\text{cyl}}}. \quad (33)$$

The value of the heat transfer coefficient is returned to the main model.

### 3 Calculation results

In this part of the paper, the distribution of an ideal leak-free compression process (L0) was determined with the assumption that there is no heat transfer between the steam and the walls of the compression chamber (HT0). In the next part of the paper, it is assumed that these processes are the reference processes.

In the subsequent calculation variants, leakage and heat transfer between the steam and the walls of the compression chamber was taken into account. These variants were to approximate the considered compression process with the real one.

The appearance of leakage of various intensity (L1–L4) and the heat transfer HT1 were assumed. In the programmed model, the inclusion of leakage and heat transfer is autonomous.

During the compression process, when the piston moved up, the compression ring aligned itself inside the piston groove in a way that caused the leakage to occur around the ring gap (Fig. 1). Under real operating conditions, the compression ring deforms around the ring gap as a result of wear and the changing distribution of the compressed gas pressure. As a consequence, leakage can occur not only in the ring gap marked in Fig. 1b. Due to the lack of specific knowledge about the real steam flow area through the compression ring, the other part of the paper used a reference flow area around the ring gap equal to  $A_{RG} = 4 \cdot 10^{-8} \text{ m}^2$  (Fig. 1). The L1 variant included leakage through a one-time flow area in the ring gap  $A_{RG}$ . L2, L3, and L4, respectively, mark the inclusion of the leakage through the flow area equal to the multiplicity of  $A_{RG}$  (multiplied by two, three and four, respectively). Table 1 comprises the analyzed calculation variants.

Table 1: Summary of the analyzed calculation variants.

Denotement	Description	General description
HT0	lack of heat transfer	theoretical compression process
L0	lack of leakage	
HT1	including heat transfer	real compression process
L1–L4	including leakage through a multiple of the flow area in the compression ring gap $A_{RG}$	

Heat transfer between the steam and the compression chamber walls occurs in the real compression process. This phenomenon was included in the variant of calculations described in the further part of the paper as HT1. The assumed temperature of the compression chamber walls for the first part of the conducted calculations was  $T_w = 120^\circ\text{C}$ .

The results presented assumed the calculation step of every 1 mm of the piston displacement. The first calculation step focused on determining the parameters of saturated steam. As a consequence of the movement of the piston towards the head, the volume of the cylinder decreased, causing an increase in the steam pressure. The pressure and steam temperature increased for the next positions of the piston.

Figure 4 shows the change of temperature in the pressure function for the variants of the calculations described above. The simulation of the compres-

sion process started with an initial steam pressure of 200 kPa. Depending on pressure, temperature changes had identical distributions for different variants of calculation. The results obtained differ in terms of final pressure. When leakage and heat transfer were excluded, the final pressure exceeded 45 MPa. When only heat transfer (L0\_HT1) was included, the final pressure was lower by 4.32 MPa than in case (L0\_HT0).

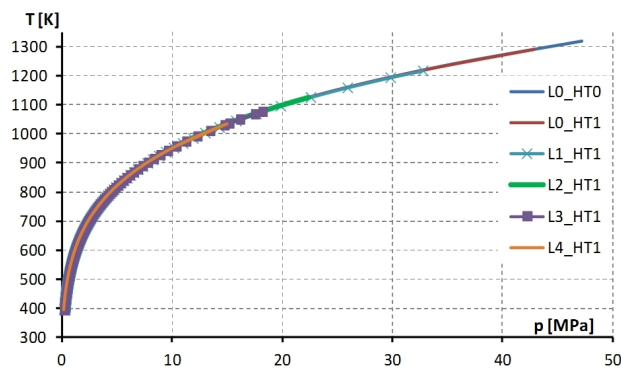


Figure 4: Distribution of the steam temperature in the pressure function for different calculation variants.

Figure 5 shows pressure changes inside the cylinder in the piston position function. Maximum pressure was limited to 30 MPa for better readability of Fig. 5. Differences in the pressure distributions for the considered calculation variants can be seen above 300 mm of the piston stroke. The pressure

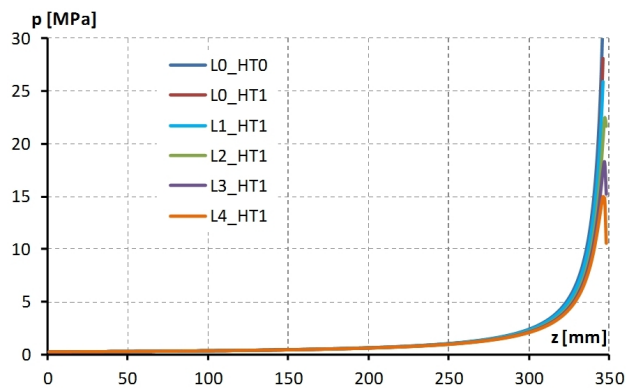


Figure 5: Steam pressure in the piston position function.

of compressed steam began to increase intensively in the last 25 mm of the piston stroke. Then, the steam density increased significantly (Fig. 6). If the steam flux flowing through the seal is too high due to the increase in density, the leakage can cause a sudden decrease in the steam pressure at the end of the compression stroke. A pressure distribution of that type can be observed in the case of variants L2\_HT1, L3\_HT1, L4\_HT1 (Fig. 5).

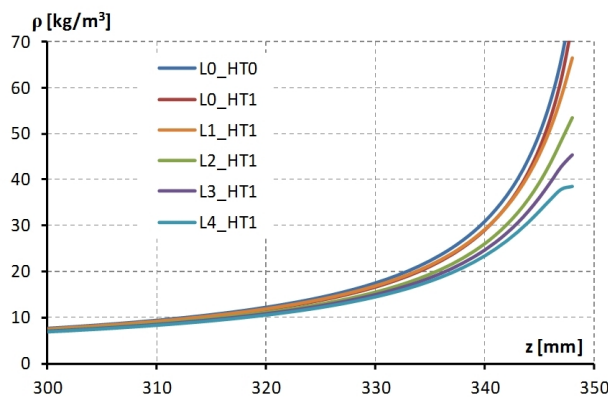


Figure 6: Steam density in the piston position function.

After the inclusion of the heat transfer and leakage (Figs. 4 and 5) the pressure and final temperature values were much lower compared to the ideal compression process (L0\_HT0).

Based on Fig. 5 and the comparison of the maximum steam pressure values at the end of the compression stroke, it can be concluded that the heat transfer effect has an impact on the final pressure of the ideal seal of the piston-cylinder assembly (L0-HT0 and L0\_HT1). By including the leakage of the value resulting from the flow through the area  $A_{RG}$  (L1) to the four times higher value (L4), the authors obtained the respective final pressure values: 32.7, 22.4, 18.2, and 14.9 MPa.

The leakage provides lower pressure and temperature, as well as the resulting lower steam density (Fig. 6). Steam density at the end of the compression stroke increased significantly slower for variants of intense leakage L3\_HT1 and L4\_HT1.

As a result of the occurrence of leakage and heat transfer to the reactor walls, a lower steam temperature was obtained along with a lower pressure. To clearly define the changes in steam temperature, it was related to the temperature obtained in the ideal compression process (L0\_HT0), that is,

adiabatic without leakage, as described by the dependency

$$\delta T = \frac{T}{T_{L0,HT0}}. \quad (34)$$

Figure 7 shows a decrease in the relative steam temperature  $\delta T$  in the piston position function. The data included in Fig. 7 shows that the only phenomenon of heat transfer from steam to the walls at temperature  $T_w = 120^\circ\text{C}$  caused a slight decrease in the relative temperature, equal to 0.0207. Leakage is a crucial factor that causes the decrease in temperature in compressed steam. The inclusion of leakage and the determination of its intensity with the use of the flow reference area decreased the relative temperature by 0.076. On the other hand, by assuming 4 times the reference surface area of the leakage transfer, the temperature decreased significantly by 0.27.

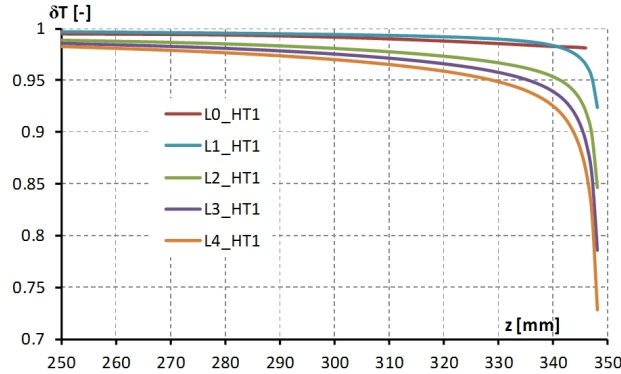


Figure 7: Relative steam temperature decrease in the piston position function.

The relative steam mass within the cylinder related to the ideal conditions (variant L0) was used to precisely define the impact of the leakage on the amount of mass contained in the cylinder (see Fig. 8):

$$\delta m = \frac{m}{m_{L0}}. \quad (35)$$

Figure 8 shows that a significant leak occurred not sooner than in the last 20 mm of the piston stroke. The 0.25 decrease in mass inside the cylinder was obtained for the leakage through the area  $A_{RG}$  (L1). The leakage through double, triple, and quadruplicity of the  $A_{RG}$  flow area (L2–L4) caused the mass to decrease by the respective values of 0.41, 0.56 and 0.67.

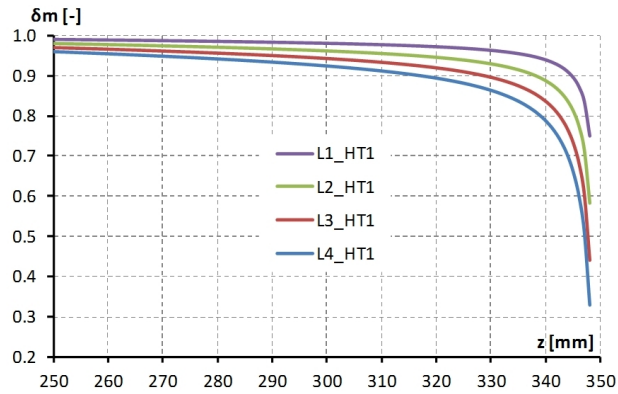


Figure 8: Relative steam mass contained in the cylinder in the piston position function.

The Reynolds number has an impact on the intensity of heat transfer, and is dependent on momentary velocity values of the piston and the steam viscosity, as defined in Eq. (12). The first local maximum of Reynolds number occurred after around 80 mm of the piston stroke and resulted from the momentary, and relatively high, piston velocity. The second maximum occurred around 325 mm of the piston stroke and was caused by the decrease in steam viscosity (Fig. 9).

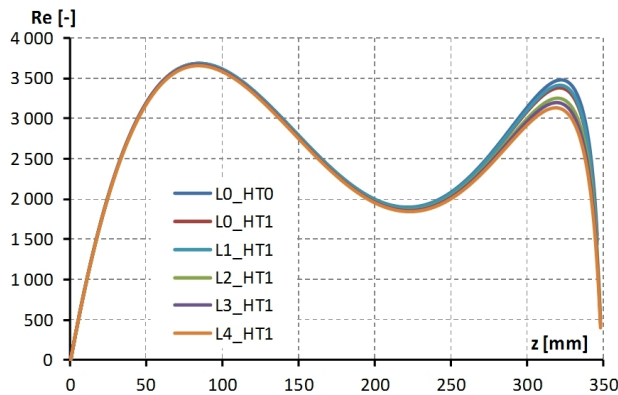
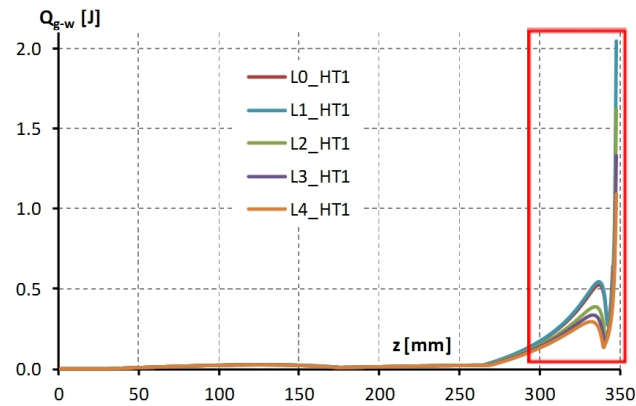


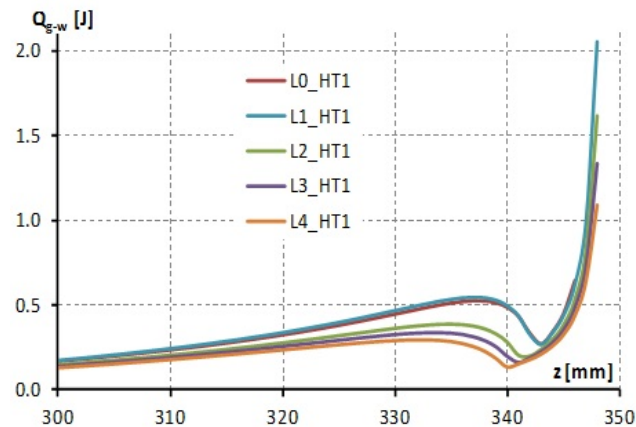
Figure 9: The Reynolds number distribution.

The intensity of gas turbulence within the reactor cylinder defined by the Reynolds number has a direct impact on the heat transfer conditions between the compressed steam and the reactor walls. In addition to the

Reynolds number, the temperature and density of compressed steam affect the heat transfer. The amount of heat transferred to the reactor walls in the first 250 mm of the piston stroke was small due to a low density of steam (Fig. 10). The intensity of the heat transfer reached the local maximum between 330 mm and 340 mm of the piston movement for the analyzed calculation variants under consideration. After 340 mm, a decrease in the intensity of heat transfer could be observed. It was a result of the decrease in the piston velocity and the Reynolds number.



(a)



(b)

Figure 10: Heat transferred by steam to the cylinder walls in individual piston positions: (a) for the whole stroke, (b) enlargement of the final part of the stroke.

At the end of the compression stroke, heat transfer resulting from an intense increase in steam density occurred in all calculation variants despite the decreasing piston velocity. Using the following dependency:

$$Q_{g-w,\text{sum}} = \sum_{i=1}^n Q_{g-w}(i), \quad (36)$$

the aggregate amount of heat transferred to the piston reactor walls in a given piston position was calculated (see Fig. 11).

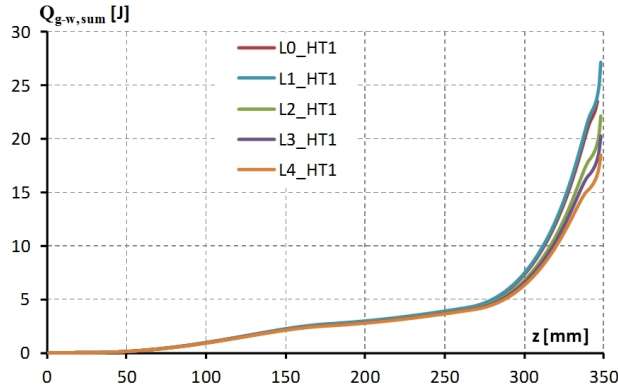


Figure 11: Aggregate amount of the heat transferred from the steam to the cylinder walls of the reactor.

The aggregate amount of heat transferred from the steam to the compression chamber walls (Fig. 11) begins to regularly increase as of 50 mm of the piston stroke.  $Q_{g-w,\text{sum}}$  values increase more rapidly as of app 280 mm of the piston stroke.

### 3.1 Analysis of the impact of the cylinder wall temperature on the heat transfer intensity

This chapter analyzes the impact of compression chamber wall temperature on direction and the value of heat transfer between steam and the walls. The calculations include the temperature of the walls ( $T_w$ ) in the range from 100°C to 200°C.

Figure 12 shows the distribution of the aggregate amount of heat transferred from the steam to the walls of the cylinder expressed by the dependency (36). The negative heat value  $Q_{g-w,\text{sum}}$  expresses the steam heated

by the cylinder walls. This phenomenon occurs in the calculation variants, in which the initial steam temperature is lower than the assumed temperature of the cylinder walls.

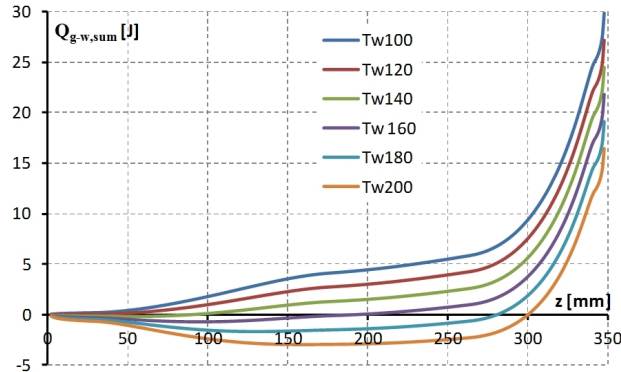


Figure 12: Aggregate amount of heat transferred from the steam to the cylinder walls of the reactor for different pre-set temperatures of the cylinder walls  $T_w$ .

In the initial stage of the stroke, steam is heated by the cylinder walls in the case where the wall temperature is equal and higher than  $140^\circ\text{C}$  (Fig. 12). Heat loss is much lower in the latter stage of the stroke when the steam temperature is higher than the wall temperature. Increasing the temperature of the cylinder walls reduced the amount of heat transferred by compressed steam. In practise, there are temperature limitations, for instance, on the cylinder wall, which result from maintaining the correct oil properties and obtaining the required oil film parameters between the compression ring and the cylinder liner.

## 4 Summary

The calculation results presented in this paper indicate that the concept of a piston reactor allows us to obtain supercritical steam parameters with a seal composed of one compression ring. For the leak tightness cases under consideration (L1–L4), the leak causes a relative drop in compressed steam mass, by a value of 0.25, 0.41, 0.56, and 0.67, consecutively. The seal in variant L1 allows us to obtain steam of pressure of 32.708 MPa and temperature of  $944^\circ\text{C}$ , and for variant L2, these parameters are equal to 21.638 MPa and  $842^\circ\text{C}$ , respectively. For cases of increased leakage (L2–

L4), at the end of the compression stroke, a pressure drop of 0.79, 3, and 4.44 MPa, respectively, was observed. This drop results from a great increase in leakage caused by a high pressure and density of steam in the last millimeters of piston displacement. The calculations were assumed to include a coefficient of flow contraction in the compression ring for the mixture of air and exhaust. To improve the accuracy of the leakage calculation model, experimental verification is needed.

For a theoretical compression process, the inclusion of heat transfer causes a drop in the final pressure by 4.32 MPa. Depending on the temperature of the walls of the compression chamber, the steam at the beginning of the compression stroke can cool or heat up. For wall temperature  $T_w = 100$  and  $120^\circ\text{C}$ , steam cools at the beginning of the compression stroke, while  $T_w = 140, 160, 180,$  and  $200^\circ\text{C}$ , steam cools at the piston displacement equal to  $z = 90$  mm, 196 mm, 282 mm and 301 mm, respectively. This stage may be crucial because of the behavior of water in a gaseous form in the initial stage of compression. It is possible to pair this model with a two-dimensional model of heat transfer in the wall of the piston reactor. This will enable the accuracy of the calculation results to increase and also allow for a more extensive analysis.

*Received 10 August 2023*

## References

- [1] Pińkowska H.: *High-temperature biomass gasification in supercritical water*. Przem. Chem. **86**(2007), 11, 1044–1050 (in Polish).
- [2] Pińkowska H.: *Low-temperature biomass gasification in subcritical and supercritical water*. Przem. Chem. **86**(2007), 7, 599–606 (in Polish).
- [3] Jitka H.: *Status report on thermal gasification of biomass and waste 2021*. IEA Bioenergy, Task 33, 2022. [https://www.ieabioenergy.com/wp-content/uploads/2022/03/Status-Report2021\\_final.pdf](https://www.ieabioenergy.com/wp-content/uploads/2022/03/Status-Report2021_final.pdf) (accessed 13 Apr. 2023).
- [4] Ashok A., Katebah M.A., Linke P., Kumar D., Arora D., Fischer K., Jacobs T., Al-Rawashdeh M.: *Review of piston reactors for the production of chemicals*. Rev. Chem. Eng. **39**(2023), 1, 1–30. doi: [10.1515/revce-2020-0116](https://doi.org/10.1515/revce-2020-0116)
- [5] Hendry D., Miller A., Jacoby W.: *Turbulent operation of a continuous reactor for gasification of alcohols in supercritical water*. Ind. Eng. Chem. Res. **51**(2012), 6, 2578–2585. doi: [10.1021/ie201887e](https://doi.org/10.1021/ie201887e)
- [6] Borowczyk T.: *Influence of charge movement in inlet manifold on combustion process in compression ignition engines*. PhD thesis, Poznan University of Technology, Poznań 2014 (in Polish).

- [7] Atakan B., Kaiser S.A., Herzler J., Porras S., Banke K., Deutschmann O., Kasper T., Fikri M., Schiefl R., Schröder D., Rudolph Ch., Kaczmarek D., Gossler H., Drost S., Bykov V., Maas M., Schulz Ch.: *Flexible energy conversion and storage via high-temperature gas-phase reactions: The piston engine as a polygeneration reactor*. *Renew. Sustain. Energy Rev.* **133**(2020), 110264. doi: [10.1016/j.rser.2020.110264](https://doi.org/10.1016/j.rser.2020.110264)
- [8] Vetter H.: *The Sulzer oil-free labyrinth piston compressor*. In: Proc. Int. Compressor Engineering Conf., Purdue 1972, paper 33, 221–228. <https://docs.lib.purdue.edu/icec/33> (accessed 14 March 2023).
- [9] Joachimiak D., Krzyślak P.: *Comparison of results of experimental research with numerical calculations of a model one-sided seal*. *Arch. Thermodyn.* **36**(2015), 2, 61–74. doi: [10.1515/aoter-2015-0015](https://doi.org/10.1515/aoter-2015-0015)
- [10] Graunke K.: *Labyrinth leakage flow in a labyrinth-piston compressor*. *Sulzer Techn. Rev.* **67**(1985), 30–33.
- [11] Feng J., Wang L., Yang H., Peng X.: *Numerical investigation on the effects of structural parameters of labyrinth cavity on sealing performance*. *Math. Probl. Eng.* **2018**(2018), 1–12. doi: [10.1155/2018/5273582](https://doi.org/10.1155/2018/5273582)
- [12] Larjola J., Honkatukia J., Sallinen P., Backman J.: *Fluid dynamic modeling of a free piston engine with labyrinth seals*. *J. Ther. Sci.* **19**(2010), 2, 141–147. doi: [10.1007/s11630-010-0141-2](https://doi.org/10.1007/s11630-010-0141-2)
- [13] Trüttnovsky K.: *Noncontacting Seals; Basics and Applications of Slot and Labyrinth Fluid-Flow Seals*. VDI-Verlag bh Dusseldorf, Publishing House of the Association of German Engineers 1964.
- [14] Melnik V.A.: *Calculating leaks in rotor-machine radial slot seals. Part 2. A method for integral slot flow rate constants*. *Chem. Pet. Eng.* **45**(2009), 11–12, 702–706. doi: [10.1007/s10556-010-9265-1](https://doi.org/10.1007/s10556-010-9265-1)
- [15] Melnik V.A.: *Calculating leaks in rotary machineradial slot seals. Part 3. Method for calculating leakstaking account of the inlet section*. *Chem. Pet. Eng.* **46**(2010), 3–4, 146–152. doi: [10.1007/s10556-010-9308-7](https://doi.org/10.1007/s10556-010-9308-7)
- [16] Melnik V.A.: *Computed universal dependence for determining leakage of media through groove seals*. *Chem. Pet. Eng.* **48**(2013), 11–12, 751–759. doi: [10.1007/s10556-013-9691-y](https://doi.org/10.1007/s10556-013-9691-y)
- [17] Joachimiak D., Krzyślak P.: *A model of gas flow with friction in a slotted seal*. *Arch. Thermodyn.* **37**(2016), 3, 95–108. doi: [10.1515/aoter-2016-0022](https://doi.org/10.1515/aoter-2016-0022)
- [18] Hao X.H., Ju Y.L., Lu Y.J.: *Experimental study on the sealing clearance between the labyrinth sealing displacer and cylinder in the 10 K G-M refrigerator*. *Cryogenics (Guildf)* **51**(2011), 5, 203–208. doi: [10.1016/j.cryogenics.2011.02.002](https://doi.org/10.1016/j.cryogenics.2011.02.002)
- [19] Asok S.P.: Sankaranarayanan K., Sundararajan T., Rajesh K., Sankar Ganeshan G.: *Neural network and CFD-based optimisation of square cavity and curved cavity static labyrinth seals*. *Tribol. Int.* **40**(2007), 7, 1204–1216. doi: [10.1016/j.triboint.2007.01.003](https://doi.org/10.1016/j.triboint.2007.01.003)
- [20] Joachimiak D., Krzyślak P.: *Analysis of the gas flow in a labyrinth seal of variable pitch*. *J. Appl. Fluid Mech.* **12**(2019), 3, 921–930. doi: [10.29252/JAFM.12.03.29074](https://doi.org/10.29252/JAFM.12.03.29074)

- [21] Chun Y.H., Ahn J.: *Effects of geometric parameters of a staggered labyrinth seal on leakage flow*. J. Mech. Sci. Technol. **37**(2023), 6, 2959–2968. doi: [10.1007/s12206-023-0522-6](https://doi.org/10.1007/s12206-023-0522-6)
- [22] Joachimiak D.: *Novel Method of the Seal Aerodynamic Design to Reduce Leakage by Matching the Seal Geometry to Flow Conditions*. Energies (Basel) **14**(2021), 23, 7880. doi: [10.3390/en14237880](https://doi.org/10.3390/en14237880)
- [23] Yuan H., Pidaparti S., Wolf M., Edlebeck J., Anderson M.: *Numerical modeling of supercritical carbon dioxide flow in see-through labyrinth seals*. Nucl. Eng. Des. **293**(2015), 436–446. doi: [10.1016/j.nucengdes.2015.08.016](https://doi.org/10.1016/j.nucengdes.2015.08.016)
- [24] Dai Z., Wang C., Zhang D., Tian W., Qiu S., Su G.H.: *Design and analysis of a free-piston stirling engine for space nuclear power reactor*. Nucl. Eng. Tech., **53**(2021), 2, 637–646. doi: [10.1016/j.net.2020.07.011](https://doi.org/10.1016/j.net.2020.07.011)
- [25] Lyubarsky P., Bartel D.: *2D CFD-model of the piston assembly in a diesel engine for the analysis of piston ring dynamics, mass transport and friction*. Tribol. Int. **104**(2016), 352–368. doi: [10.1016/j.triboint.2016.09.017](https://doi.org/10.1016/j.triboint.2016.09.017)
- [26] Wolff A., Koszałka G.: *Influence of engine load on piston ring pack operation of an automotive IC engine*. Combust. Engines **190**(2022), 3, 88–94. doi: [10.19206/CE-141737](https://doi.org/10.19206/CE-141737)
- [27] Wolff A.: *Modelling of flow phenomena of the system piston-rings-cylinder of an internal combustion engine*. Prace Naukowe Politechniki Warszawskiej. Mechanika **251**. Oficyna Wydawnicza Politechniki Warszawskiej, Warszawa 2013 (in Polish).
- [28] Shipeng W., Xuexing D., Junhua D., Jingmo W.: *Steady State Characteristics of Spiral Groove Floating Ring Gas Film Seal Considering Temperature Viscosity Effect*. J. Appl. Fluid Mech. **16**(2023), 4, 891–904. doi: [10.47176/jafm.16.04.1432](https://doi.org/10.47176/jafm.16.04.1432)
- [29] Kretzschmar H.-J., Wagner W.: *International Steam Tables. Properties of Water and Steam based on the Industrial Formulation IAPWS-IF97*. Springer, Vieweg Berlin, Heidelberg 2019. doi: [10.1007/978-3-662-53219-5](https://doi.org/10.1007/978-3-662-53219-5)
- [30] Brunner G.: *Hydrothermal and Supercritical Water Processes*. **5**, Elsevier, 2014.